

Relative Comparison of Cathode Polarizations in Solid Oxide Fuel Cells Using the Spreading Concept in AC 2 Point Impedance Spectroscopy

Byung-Kook Lee, Eui-Hyun Kim, and Jin-ha Hwang[†]

Department of Materials Science and Engineering, Hongik University, Seoul 121-791, Korea

(Received January 15, 2013; Revised February 17, 2013; Accepted February 20, 2013)

ABSTRACT

A modified two-point impedance spectroscopy technique exploits the geometric constriction between an electrolyte and a cathode with an emphasis on semispherical-shaped electrolytes. The spatial limitation in the electrolyte/electrode interface leads to local amplification of the electrochemical reaction occurring in the corresponding electrolyte/electrode region. The modified impedance spectroscopy was applied to electrical monitoring of a YSZ (Y_2O_3 -stabilized ZrO_2)/SSC ($Sm_{0.5}Sr_{0.5}CoO_3$) system. The resolved bulk and interfacial component was numerically analyzed in combination with an equivalent circuit model. The effectiveness of the "spreading resistance" concept is validated by analysis of the electrode polarization in the cathode materials of solid oxide fuel cells.

Key words : Fuel Cells, Cathodes, Impedance Spectroscopy, Interfaces, Electrochemical Polarization

1. Introduction

Solid oxide fuel cells (SOFCs) are recognized as highly efficient electrochemical conversion systems in which oxygen and hydrogen are employed as the oxidant and the fuel, respectively, to generate high-capacity electric power.^{1,2)} SOFCs have continued to garner extensive academic and industrial interest due to their high system operation efficiency and environmentally benign features including less pollution than the use of fossil fuels. The performance of SOFCs is significantly affected by the physiochemical and microstructural features of the constituent components, i.e., the electrolyte, cathode, anode, sealing materials, and the interconnect. The electrochemical loss is largely related to both the ohmic contribution originating from the above-mentioned cell components and the interfacial polarizations between the electrolyte and electrode, i.e., the cathode or the anode with regard to a given electrolyte.

In particular, cathode polarization has a critical impact on control of the output characteristics of SOFCs, e.g., the open circuit voltage and maximum power density. Enhancement of the cathodic behavior has been achieved by sophisticated design of the cathode materials and processing methods. LSM ($La_{1-x}Sr_xMnO_3$) materials have been extensively investigated either as a single-phase component or as LSM-based multiphase mixtures.³⁻⁶⁾ However, the LSM cathode is known to be a poor electronic conductor despite the chemical stability of the YSZ (Y_2O_3 -stabilized ZrO_2) electrolyte,

and consequently must be mixed with ionic conductors. Unlike LSM-based materials, the newly reported $Sm_xSr_{1-x}CoO_3$ (SSC) materials have been recognized as excellent cathode components due to the high degree of conduction that can be achieved by admixture with ionic conductors, with consequent significant enhancement of the cathodic performance.^{7,8)} The optimized polarization losses at the electrode should be integrated into highly conductive ionic conductors in order to maximize the SOFC performance. Unfortunately, no appropriate tool for evaluating the cathode polarization relative to other candidate materials and for optimizing the materials and/or processing has been developed thus far.

The acquisition of information on electrode polarization requires the simultaneous measurement of both the electrolyte and electrode contributions. Unlike conventional three-point impedance spectroscopy, the current work proposes a modified approach using ac two-point electrode impedance spectroscopy involving deliberately limited contact between the electrode and electrolyte with the aim of quantifying the normalized polarization with regard to a given electrolyte. The current work reports the electrode polarization of a mixed conduction material (SSC) in response to variation of the reference electrolyte (YSZ). The implications of the modified impedance spectroscopy technique are discussed with special emphasis on high-performance solid oxide fuel cells.

2. Experimental Procedures

Yttria-stabilized zirconia (YSZ, Tosoh, 8Y, Japan) was chosen as a reference electrolyte in this work. After full-densification at high temperature, the YSZ electrolyte was machined into a semispherical shape, as shown in Fig. 1, where

[†]Corresponding author : Jin-ha Hwang
E-mail : jhwang@wow.hongik.ac.kr
Tel : +82-2-320-3069 Fax : +82-2-333-0127

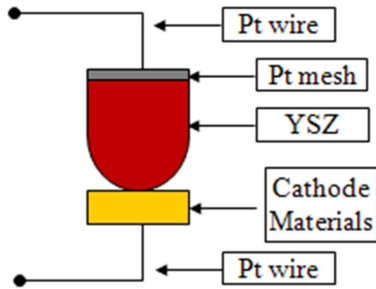


Fig. 1. Schematic diagram demonstrating geometrical constriction between the YSZ electrolyte and cathode employed for ac two-point impedance spectroscopy.

one side of the electrolyte was of semispherical shape and the other was maintained in a cylindrical form with a flat upper surface. The upper portion of the electrolyte was connected to platinum lead wires using a Pt-paste and Pt-meshes in order to provide intimate adhesion for optimized electroding. The YSZ component was sequentially treated at 800°C for 1 h in an electric furnace.

The SSC ($\text{Sm}_{0.5}\text{Sr}_{0.5}\text{CoO}_3$) discs were presintered at 800°C in order to provide the minimum mechanical strength required for installation into the measuring apparatus. The YSZ semispherical fixture and the SSC ceramic disc were loaded into spring-loaded alumina fixtures. After aligning the SSC discs in the measurement fixture, the measurement apparatus was heated to the actual sintering temperature of 950°C, mimicking the actual contact conditions between an electrolyte (YSZ) and a cathode (SSC) during the fabrication of SOFC modules.

Temperature-dependent impedance spectra were collected

in a temperature range from 600°C to 800°C using a frequency-response analyzer at an oxygen partial pressure ranging from 1 to 10^{-4} atm (including air), with an oscillating amplitude of 25 mV. The impedance spectra were acquired in a logarithmic manner between 1 MHz and 0.01 Hz with 10 points per decade. The measured impedance spectra were analyzed using an equivalent circuit model.

3. Results and Discussion

When a semispherical YSZ electrolyte is positioned onto the cathode materials, as shown in Fig. 1, the electrode configuration forms a geometrically limited contact between the YSZ electrolyte and cathode material (SSC). The geometrically narrow contact produces resistance in the ionic electrolyte, and the corresponding electrode polarization increases dramatically due to the significant reduction in the contact area at the electrolyte/electrode interface. Such electrical phenomena can be interpreted in terms of spreading resistance.^{9,10} Although the “spreading resistance” concept has been widely utilized in electron-based semiconductors, an identical concept can be applied to ionic conducting systems such as ionically operating solid oxide fuel cells.¹¹⁻¹⁴ As expected from the limited contact illustrated in Fig. 1, the geometric constriction increases the related resistance and decreases the corresponding capacitance according to the following equation:^{9,10,15}

$$R_c = \rho_{\text{bulk}} \left(\frac{1}{4a} \right) \quad (1)$$

where R_c is the spreading resistance due to the geometrical constriction at the electrolyte/electrode interface, σ is the

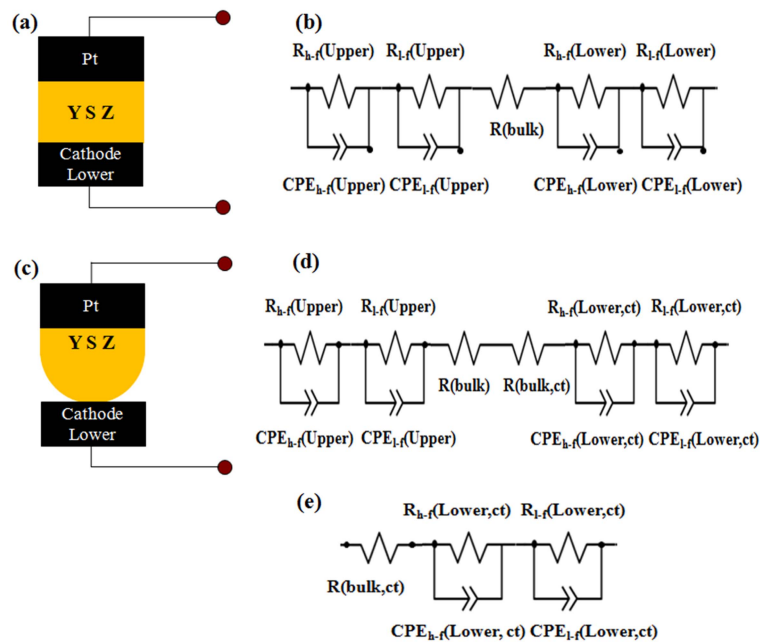


Fig. 2. Schematic cell descriptions (a, c) and their equivalent circuit models (b, d, and e). Detailed cell structures of (a) parallel electrode and (c) unparallel electrode configurations involving a geometrical constriction between electrode and an electrolyte. The corresponding equivalent circuit models are shown in (b) and (d). (e) shows the resultant approximation of Fig. 4(d).

conductivity of the electrolyte, and a is the radius of the contact area.^{9,10} Furthermore, the corresponding capacitance is given by the following equation:

$$C_c = 4\epsilon\epsilon_0 a \quad (2)$$

where C_c is the capacitance due to geometric constriction at the electrolyte/electrode interface, ϵ is the relative dielectric constant, and ϵ_0 is the vacuum dielectric constant.

Conventional two-point electrode impedance spectroscopy incorporates a two parallel electrode geometry, as shown in Fig. 2(a). The corresponding equivalent circuit model can be described as shown in Fig. 2(b), where the bulk resistance component is connected to two RC circuits originating from two interfaces. However, the overall impedance spectra cannot be resolved explicitly due to the overlapping electrode contributions of the electrodes, i.e., the upper and lower electrodes. In other words, discrete contributions from each electrode cannot be deconvoluted due to the similar magnitudes of their corresponding time constants. Furthermore, the high-frequency bulk resistance is typically small, in a range of several ohms, and is the sum of the ohmic electrolyte and electrode resistances. However, the asymmetric electrode configuration (e.g., the limited contact between an electrode and electrolyte) shown in Fig. 2(c) alters the numerical polarization parameters, as shown in Fig. 2(d). The geometrical constriction leads to additional spreading resistance within the YSZ electrolyte, in addition to the amplified electrode contribution originating from the electrode polarization near a pointed contact point. The equivalent “spreading resistance” is much larger than the initial resistance (on the order of several ohms). Consequently, the resultant bulk and electrode polarization can be simplified, as shown in Fig. 2(e), and the resultant impedance spectra exhibit the bulk ionic contribution and the electrode polarization adjacent to the geometrically constricted point presented in Fig. 2(c). The actual impedance spectra are shown as a function of temperature and oxygen partial pressure in Fig. 3. The empirical impedance spectra of Fig. 3 can be systematically analyzed based on the proposed equivalent circuit modeling of Fig. 2(e). The current study assumes that there are two RCPE components depending on the intermediate and low frequency regimes, i.e., $(R_{h-f}CPE_{h-f})(R_{l-f}CPE_{l-f})$, where the subscripts “h-f” and “l-f” denote the high-frequency and low-frequency components in the electrode-related impedance spectrum portions. In the symmetric and parallel electrode configurations, two electrode responses are superimposed, leading to one set of interfacial electrode responses, precluding the possibility of separating the constituent electrodes, i.e., the upper and lower electrodes. In contrast, the asymmetric electrode configuration induces a significant imbalance. However, the contact-related (RCPE) component is still close to that of the parallel/large-area electrode. The overall impedance spectrum is largely controlled by the RC contributions originating from the geometric constriction due to the dissimilar natures of the resis-

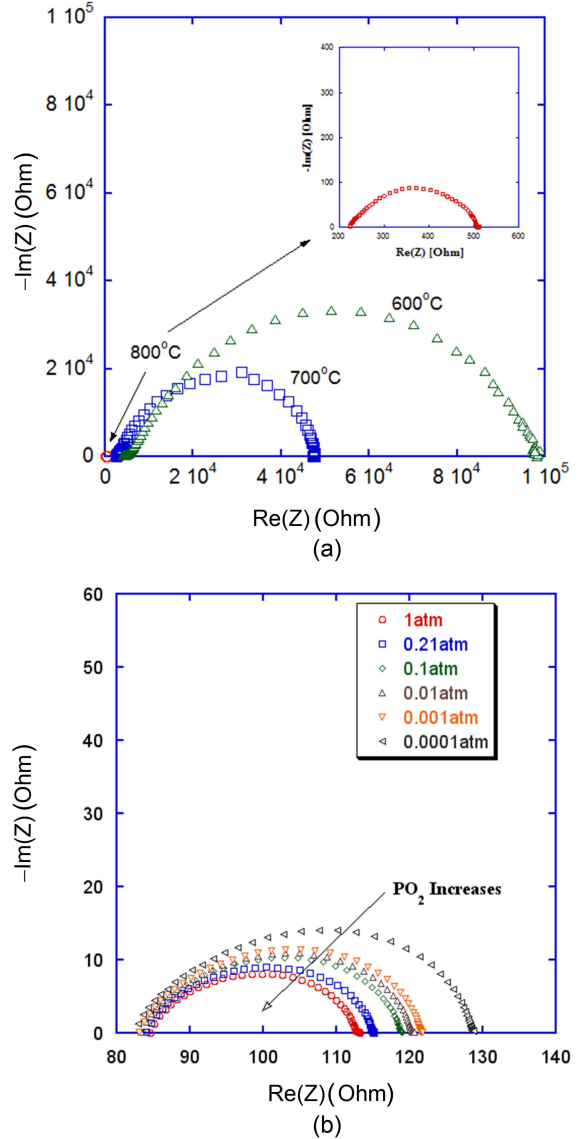


Fig. 3. Impedance spectra: (a) impedance spectra as a function of temperature and (b) impedance spectra as a function of oxygen partial pressure using $\text{Sm}_{0.5}\text{Sr}_{0.5}\text{CoO}_3$ as cathode materials.

tances and capacitances in their serial connection structure (see Fig. 2(e)).

The detailed information of both bulk and electrode contributions allows for determination of the normalized cathode polarizations (the ratio of $(R_{h-f} + R_{l-f})$ to R_0) with regard to a given electrolyte.

$$\begin{aligned} \text{Normalized Polarization} &= \\ &= (\text{Total Electrode Polarization}) / (\text{Spreading Resistance}) \quad (3) \\ &= R_t / R_0 = (R_{h-f} + R_{l-f}) / R_0 \end{aligned}$$

The normalized polarization indicates the polarization loss with regard to the specific electrolyte, allowing for a relative comparison among various cathode materials applied to the specified electrolyte. As the normalized polarization

Table 1. Analyzed Resistance Values of Bulk (R_0) and Interfacial Components (R_{h-f} and R_{l-p}) Related to Cathode Materials as a Function of Oxygen Partial Pressure Obtained at 800°C

Oxygen Partial Pressure (atm)	R_0 (Ω)	R_{h-f} (Ω)	R_{l-p} (Ω)	R_t (Ω)	R_t/R_0
1	85.67	5.03	22.14	27.17	0.317
0.21	85.19	5.582	24.28	29.862	0.350
0.1	84.72	6.062	28.17	34.232	0.404
0.01	84.43	6.273	29.78	36.053	0.427
0.001	84.22	6.384	31.08	37.464	0.445
0.0001	85.36	8.25	36.95	45.2	0.541
1 (LSM)*	182.2	24.38	439.4	463.78	2.545

*Reference [17]

Table 2. Analyzed Resistance Values of Bulk (R_0) and Interfacial Components (R_{h-f} and R_{l-p}) as a Function of Temperature Related to Cathode Materials Obtained in Ambient Conditions

Temperature ($^{\circ}$ C)	R_0 (Ω)	R_{h-f} (Ω)	R_{l-p} (Ω)	R_t (Ω)	R_t/R_0
800	85.19	24.28	5.582	29.862	0.350
700	208.60	129.60	339.70	469.3	2.250
600	755.90	1203.0	7910.0	9113	12.056

becomes smaller, the cathodic performance is accordingly enhanced. In other words, minimization of the normalized polarization reduces the effective loss across the unit cells, improving the output performance, i.e., the resultant power. As shown in Fig. 3(b), the bulk response, i.e., the high-frequency intercept, is independent of oxygen partial pressures with much larger resistance values than those obtained with the parallel electrode configuration. The analyzed parameters are presented in Tables 1 and 2 and Fig. 4. The temperature-dependent information allows for calculation of the activation energy related to the YSZ bulk component, which was found to be 0.97 eV. The bulk activation energy reportedly ranges from 0.80–1.0 eV, which is in reasonable agreement with the value determined in the current study.^{15,17)} The activation energies of R_{h-f} and R_{l-p} are calculated to be 1.66 and 2.98 eV, respectively. In particular, R_{l-p} increases most significantly with decreasing temperature, likely due to a reduction in the electrochemical reaction involving oxygen transport. The oxygen partial pressure affects the charge transport kinetics, and the low oxygen partial pressure is believed to increase the corresponding polarization loss. The defect chemistry of $\text{Sm}_{0.5}\text{Sr}_{0.5}\text{CoO}_3$ cathode materials may be responsible for the reduction in ionic conductivity at high oxygen partial pressure. However, the current observation appears to support a much higher contribution from the polarization loss reduction in mixed conducting cathodes compared to the counter-effect due to the low ionic conductivity at high oxygen partial pressure.

Our previous work on LSM materials indicated a much higher polarization value than that of mixed conducting SSC materials: the normalized electrode polarization of an LSM-based cathode is 2.545 and that of an SSC cathode is calculated to be 0.345 under identical temperature and oxygen partial pressure conditions, indicating that SSC is the most appropriate cathode material with regard to the YSZ

electrolyte.¹⁸⁾ In particular, given that the cathode materials provide sufficient porosity allowing for the rapid diffusion in oxygen molecules, the current two (*RCPE*) components are believed to be associated with the adsorption/desorption process on the surface of the cathode electrode and ionic conduction within the mixed conducting materials, i.e., SSC rather than the diffusional contribution of oxygen molecules, based on work by Koyama *et al.*⁸⁾

Baker *et al.*¹⁹⁾ considered spreading resistance concepts and dealt with the geometric constriction in terms of electrodes, unlike the current work. The spreading resistance concept was applied in their study only to explain their results regarding the electrodes based on estimation of the electrode only. Accordingly, the current normalized polarization concept can provide a relative comparison among cathode materials. The current methodology is believed to be more universal than other previously reported methods. The modified impedance spectroscopy approach can be applied to various types of electrolytes, regardless of temperature or oxygen partial pressure. A more detailed numerical approach will be employed in a forthcoming study.

4. Conclusions

The geometric restriction implemented in this study allows quantitative determination of the cathode polarizations due to a single electrode with regard to a specified electrolyte. The measured impedance information was explained based on a “spreading resistance” concept and the apparent bulk and interfacial contributions were determined to originate solely from the geometrically limited contact. The corresponding bulk and interfacial contributions were analyzed with regard to temperature and oxygen partial pressure using a simplified equivalent circuit, $R_0(R_{h-f}CPE_{h-f})(R_{l-p}CPE_{l-p})$, involving resis-

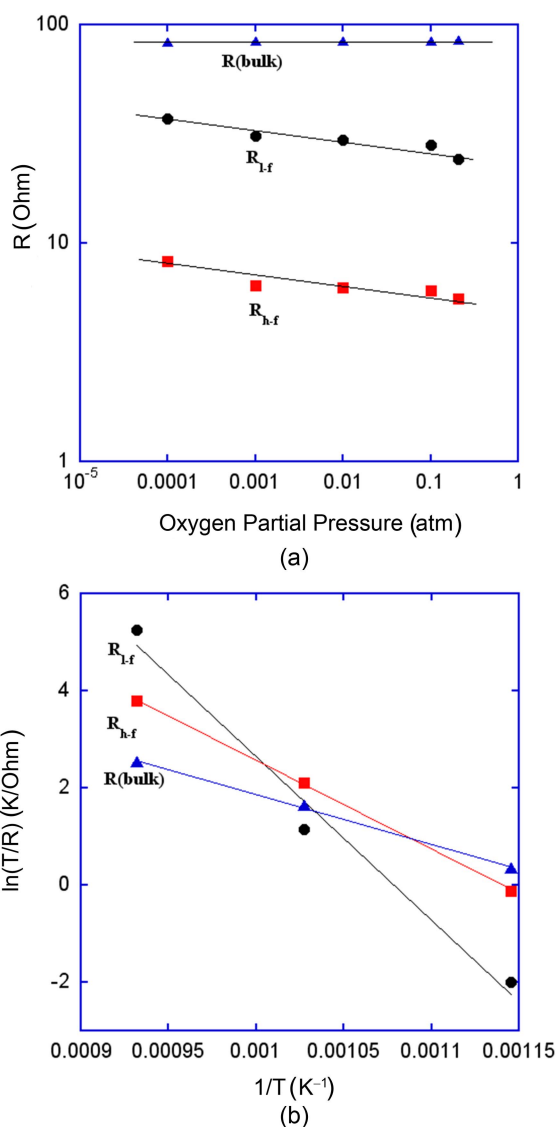


Fig. 4. Temperature-dependence and oxygen partial pressure dependence of analyzed bulk and interfacial components.

tors and constant phase elements.

Acknowledgment

This work was supported by a grant from the Fundamental R&D Program for Core Technology of Materials funded by the Ministry of Knowledge Economy, Republic of Korea.

REFERENCES

1. B. C. H. Steele and A. Heinzel, "Materials for Fuel-Cell Technologies," *Nature*, **414** 345-52 (2001).
2. N. Q. Minh, "Ceramic Fuel Cells," *J. Am. Ceram. Soc.*, **76**

- [3] 563-88 (1993).
3. J. Van Herle, A. J. MacEvoy, and K.R. Thampi, "A Study on the $\text{La}_{1-x}\text{Sr}_x\text{MnO}_3$ Oxygen Cathode," *Electrochim. Acta*, **41** [9] 1447-54 (1996).
4. F. H. Van Heuveln and H. J. M. Bouwmeester, "Electrode Properties of Sr-Doped LaMnO_3 on Yttria-Stabilized Zirconia," *J. Electrochem. Soc.*, **144** 134-40 (1997).
5. J. Mizusaki, H. Tagawa, K. Tsuneyoshi, and A. Sawata, "Reaction Kinetics and Microstructure of the Solid Oxide Fuel Cells Air Electrode $\text{La}_{0.6}\text{Ca}_{0.4}\text{MnO}_3/\text{YSZ}$," *J. Electrochem. Soc.*, **138** 1867-73 (1991).
6. E. Ivers-Tiffée, A. Weber, and D. Herbristrit, "Materials and Technologies for SOFC-Components," *J. Eur. Ceram. Soc.*, **21** 1805-11 (2001).
7. C. Xia, W. Rauch, F. Chen, and M. Liu, " $\text{Sm}_{0.5}\text{Sr}_{0.5}\text{CoO}_3$ Cathodes for Low-Temperature SOFCs, Solid State Ionics," **149** [1-2] 11-19 (2002).
8. M. Koyama, C. J. Wen, T. Masuyama, J. Otomo, H. Fukunaga, K. Yamada, K. Eguchi, and H. Takahashi, "The Mechanism of Porous $\text{Sm}_{0.5}\text{Sr}_{0.5}\text{CoO}_3$ Cathodes Used in Solid Oxide Fuel Cells," *J. Electrochem. Soc.*, **148** [7] A795-801 (2001).
9. J. Newman, "Resistance for Flow of Current to a Disk," *J. Electrochem. Soc.*, **113** 501-02 (1966).
10. R. Holm, *Electric Contacts: Theory and Application*, 4th Edition, Springer-Verlag, New York, 1967.
11. R. Brennan and D. Dickey, "Determination of Diffusion Characteristics Using Two-and Four-Point Probe Measurements," *Solid State Technol.*, **27** [12] 125-32 (1984).
12. R. G. Mazur and D. H. Dickey, "A Spreading Resistance Technique for Resistivity Measurements on Silicon," *J. Electrochem. Soc.*, **113** 225-59 (1966).
13. A. Casel and H. Jorke, "Comparison of Carrier Profiles from Spreading Resistance Analysis and from Model Calculations for abrupt Doping Structures," *Appl. Phys. Lett.*, **50** 989 (1987).
14. J. Fleig, F. S. Baumann, V. Brichzin, H.-R. Kim, J. Jamnik, G. Cristiani, H.-U. Habermeier, and J. Maier, "Thin Film Microelectrodes in SOFC Electrode Research," *Fuel Cells*, **6** [3-4] 284-92 (2006).
15. W. R. Smythe, *Static and Dynamic Electricity*, p. 25, 3rd Edition, McGraw-Hill, New York, 1950.
16. P. Mondal and H. Hahn, "Investigation of the Complex Conductivity of Nanocrystalline Y_2O_3 -Stabilized Zirconia," *Ber. Bunsenges Phys. Chem.*, **101** [11] 1765-68 (1997).
17. P. S. Manning, J. D. Sirman, and J. A. Kilner, "Oxygen Self-Diffusion and Surface Exchange Studies of Oxide Electrolytes Having the Fluorite Structure," *Solid State Ionics*, **93** 125-32 (1997).
18. B. K. Lee, J. Y. Lee, H. Y. Jung, J. H. Lee, and J. H. Hwang, "Monitoring of the LSM/YSZ Interface in SOFCs Using Limited-Contact Geometry in Impedance Spectroscopy," *Solid State Ionics*, **179** [21-26] 955-59 (2008).
19. R. Baker, J. Guindet, and M. Kleitz, "Classification Criteria for Solid Oxide Fuel Cell Electrode Materials," *J. Electrochem. Soc.*, **144** 2427-32 (1997).